Alternative method for the evaluation of the abrasive water-jet cutting of grey cast iron

A.W. Momber *, R. Kovacevic, H. Kwak [1]

University of Kentucky, Center for Robotics and Manufacturing Systems, Lexington, KY 40506, USA

Industrial summary

A method has been developed and used for estimating the erosion debris size, D, and the contact number, C_N, for material erosion by abrasive water jets with velocities of up to 370 m/s. Based on abrasive water-jet cutting tests on grey cast iron samples, and on measurements of the particle sizes of the removed material debris, the contact number is calculated as the ratio of the number of removed material particles to the number of impacting abrasive particles, the contact numbers ranging between $C_N = 3$ and $C_N = 11$. It is found that the contact number increases linearly with the abrasive particle velocity in the medium velocity range, but for very low and very high abrasive velocities the contact number is less influenced by the abrasive velocity. A model is developed for approximating the contact numbers for various cutting conditions. Estimated high contact numbers suggest that a complex impact erosion process may occur which is associated with the formation of a microcrack network by solid particle impact and the widening of the cracks by a high-speed water flow entering the crack. © 1997 Elsevier Science S.A.

Keywords: Abrasive water-jet cutting; Grey cast iron; Particle size

1. Introduction

As a new manufacturing process, abrasive water-jet machining has been very effective in machining difficult-to-machine materials. This machining technique is one of the most recently introduced machining methods. Abrasive water jetting is used for cutting a wide range of materials, including ceramics [1,2], and composite materials [3,4]. As shown in Ref. [5], abrasive water jets also have the potential for three-dimensional machining. On the basis of jet generation, abrasive water jets can generally be categorized as injection jets (AIJ) or suspension jets (ASJ). For practical applications, AIJs are more commonly used. For this type of jet, the pump pressure ranges between 100 and 400 MPa. An AIJ is formed by accelerating small abrasive particles (garnet, aluminum oxide, silicon carbide) through contact with a high velocity plain water jet. A typical abrasive grain diameter is 400 μm. The high pressure water is converted into a high velocity water jet as

it flows through an orifice on the top of the abrasive cutting head. The abrasives enter the cutting head through a separate inlet. The mixing between abrasives, water and air takes place in a mixing chamber, and the acceleration process occurs in an acceleration tube, or abrasive water-jet nozzle. The abrasives leave this nozzle at velocities of several hundred meters per second. A high number of abrasive particles (10^5/s) leads to a high-frequency impingement on the material being processed. The intensity and the efficiency of the cutting process depend on several process parameters, such as pump pressure, orifice diameter, traverse rate, standoff distance, abrasive flow rate, abrasive type, and mixing chamber geometry [6].

The velocities of the impacting abrasive particles, w_P, can be calculated using the following procedure. Based on a momentum balance in the mixing nozzle it can be shown that:

$$w_P = \alpha \frac{w_0}{1 + \dfrac{M_P}{M_W}} \tag{1}$$

where α is a mixing and acceleration efficiency coefficient. For the estimation of the water-jet velocity, w_0, Bernoulli's law can be used, which yields:

* Corresponding author. WOMA Apparatebau GmbH, Werthauer Strasse 77-79, 47226 Duisburg, Germany. Fax: +49 2065 304 200.
[1] Present address: Samsung Electro-Mechanics Co., Ltd, Seoul, South Korea.

$$w_0 = \mu \sqrt{\frac{2p}{\rho_w}} \tag{2}$$

here μ is an orifice efficiency coefficient. The abrasive particle velocity, w_p, can now be calculated using Eq. (3):

$$w_p = \frac{\alpha\mu \sqrt{\frac{2p}{\rho_w}}}{1 + \frac{4\dot{M}_p}{\pi\mu\sqrt{2p\rho_w}d_w^2}} \tag{3}$$

During the material removal process, a part of the abrasive water-jet input energy is consumed by the workpiece and contributes to the machining process. As shown in Refs. [7,8] for brittle materials, only a small amount of the abrasive water-jet input energy is used directly to create the target material wear particles, the rest of the energy being dissipated by different mechanisms, such as friction, plastic deformation, and damping [9]. A considerable portion of the input energy is carried by the mixture of abrasives, water, and wear particles after it leaves the workpiece [10,11]. The energy dissipated in the workpiece significantly influences the machining efficiency, such as the depth of cut and the material removal rate, as well as the machining quality, such as surface roughness and striation formation. It was shown, for example, in Ref. [12] that the erosion rate in abrasive water-jet cutting increases linearly with the kinetic energy of the abrasive particles. The greater is the available energy to feed the dissipation process, the greater is the possible depth of cut in the specimen. For a given depth of cut these relations may determine the quality of the cut surface. In relation to the surface quality parameters, it has been proposed in Ref. [13] that the smooth cutting zone in the upper part of the cut, which is typically characterized by surface roughness, may be the result of excessive jet energy. There is an excess of jet energy compared with the energy required for the material removal which contributes to the generation of a comparatively smooth cutting surface. A very similar approach was proposed recently in Ref. [14] suggesting that the available local kinetic energy of the abrasive particles determines the quality of the abrasive water-jet cutting process, especially the formation of striation marks on the cut surface on the lower part of the cut. In Ref. [14] a physical model for the striation formation process was developed and verified experimentally. Also, a significant relationship between the kinetic energy of the abrasive particle and the transition cut depth between smooth cutting zone and rough cutting zone was found. In other words, if the abrasive's kinetic energy is below a given level, the striation formation process will be introduced. For local energy levels beyond this value the excessive energy contributes to the smoothing of the surfaces as proposed in Ref. [13]. In Refs. [15,16] a

mathematical model for the estimation of the local abrasive water-jet energy is introduced.

An alternative approach to treat problems related to the material removal process in materials subjected by abrasive water jets is to conduct quantitative investigations on the material particles removed by the high-speed abrasive particle erosion. As shown in Ref. [7], the removed grain samples contain information that can be used successfully to analyse material-removal processes. The subject of this paper is the application and estimation of the so-called 'contact number', C_N, which is used successfully to evaluate erosion processes in the field of dry solid particle erosion [17-19] to the abrasive water-jet cutting process.

The behaviour of the cast iron is assumed to be that of a brittle material. Grey cast iron can generally be considered as a two-phase material containing a hard matrix and graphite as a softer second phase. In the grey cast iron, the graphite flakes which can be considered essentially as sharp cracks, inhibit deformation of the normally ductile ferrite and produce a very brittle behaviour. This assumption is supported by experiences in the solid impact and cavitation erosion and impact wear of cast irons. Okada et al. [20] noticed long erosion cracks occurring in grey cast iron because of the severe notching action of the graphite in grey cast iron samples subjected to cavitation erosion. A brittle behaviour of cast iron combined with features of ductile erosion was found in Refs. [21,22] for multiple impact testing. In the two latter references significant features of extensive carbide fracture, de-cohesion at the grain-matrix interface, matrix fracture, and spall formation in a narrow zone just below the impacted surface are reported. Laird et al. [23] suggested a merging of crack fronts which originated in pre-existing fractured carbides and resulted in spalling. Radial cracking and fracture in cast iron were also found during the high-speed impact of projectiles [24]. In contrast, Balan et al. [25] observed a maximum solid particle erosion of grey cast iron at low impact angles, indicating a ductile erosion response. Nevertheless, they observed subsurface cracking at impact angles of 90°.

2. Contact number estimation

In erosion processes, the contact number, C_N, is defined as the ratio of the number of removed wear particles to the number of impacting abrasive particles [18], as given in Eq. (4):

$$C_N = \frac{N_D}{N_P} \tag{4}$$

The number of particles removed from the target specimen, N_D, can be estimated by Eq. (5) as the ratio of the mass of the removed material to the mass of a single removed wear particle:

$$N_{\text{D}} = \frac{M_{\text{D}}}{m_{\text{D}}} \tag{5}$$

Assuming the shape of the removed wear particles is a mixture of spheres, cubes, tetrahedrons, and octahedrons leads to Eq. (6):

$$N_{\text{D}} = \frac{V_{\text{D}}}{0.523 D^3} = \frac{6 V_{\text{D}}}{\pi D^3} \tag{6}$$

The number of the impacting abrasive particles, N_{P}, can be calculated by Eq. (4), based on the applied abrasive flow rate, $\dot{M}_{\text{P}}$, and the time of exposure, t_{E}:

$$N_{\text{p}} = \frac{\dot{M}_{\text{P}} t_{\text{E}}}{m_{\text{P}}} (1 + \chi) \tag{7}$$

where the parameter χ characterizes the comminution of the abrasive particles during the mixing and acceleration process which was reported in Refs. [26,27] and leads to an increase in the number of impacting abrasive particles on the erosion site. The time of exposure can be estimated by $t_{\text{E}} = L_{\text{K}}/v_{\text{T}}$ where L_{K} is the length of the cut. Assuming the shape of the abrasive particles to be spherical, Eqs. (4)–(7) yield:

$$C_{\text{N}} = \frac{V_{\text{D}} v_{\text{T}} d_{\text{P}}^3 \rho_{\text{P}}}{D^3 \dot{M}_{\text{P}} L_{\text{K}} (1 + \chi)} \tag{8}$$

Eq. (8) contains some important process parameters, such as the traverse rate, v_{T}, and the abrasive flow rate, $\dot{M}_{\text{P}}$. The unknown parameters in this equation are the average particle diameter of the removed target material, D, the average abrasive grain diameter, d_{P}, and the volume of the removed material, V_{D}. It is important to note that the values of these latter parameters depend on the traverse rate, v_{T}, the abrasive particle velocity, v_{P}, and the abrasive feed rate, $\dot{M}_{\text{P}}$.

Using methods of grain-size distribution analysis [28], the average diameter of a grain collection can be estimated by Eq. (9):

$$\bar{D} = \frac{V_{\text{M}} \psi \int_{d_{\text{U}}}^{d_0} d^3 f(D) \, \mathrm{d}D}{\rho_{\text{M}} \int_{d_{\text{U}}}^{d_0} d^2(D) \, \mathrm{d}D} \tag{9}$$

Therefore, the average grain diameters D and d_{P} can be calculated based on a sieve analysis of the removed material samples as well as on the used abrasive material. In order to estimate the average grain diameters of the abrasive and the target materials, and the volume removal on the material sample, cutting experiments, particle collection and sieve analyses were carried out as described in Section 3.

3. Experimental

Fig. 1 shows the flow chart of the experimental work that was done during the investigation. For cutting the
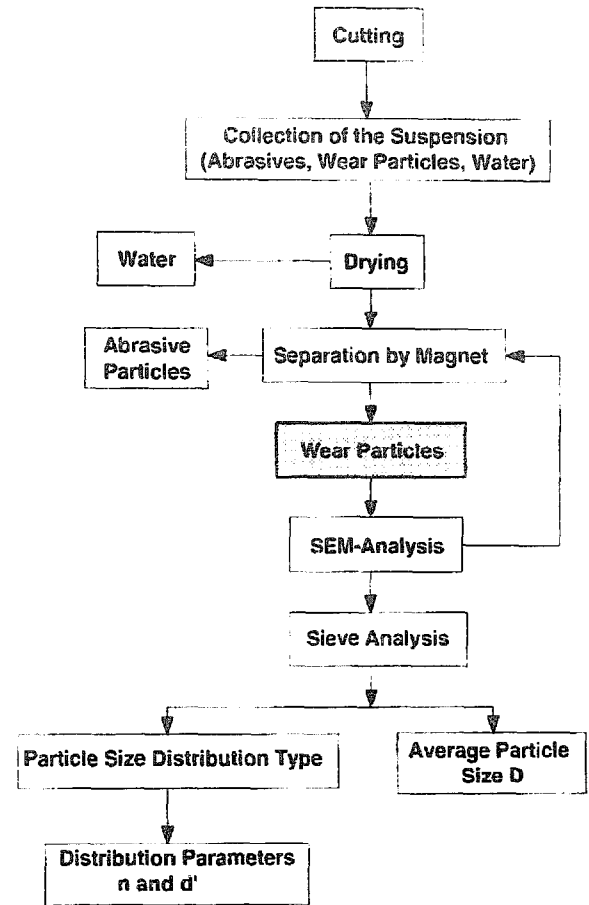

Fig. 1. Flow chart of the experimental work.

specimens, an abrasive water-jet system was used which consists of a high-pressure intensifier pump, an AWJ cutting head, an abrasive storage and metering system, a catcher tank, and an x-y-z positioning table controlled by a CNC controller. Using a micrometer screw, it was possible to adjust the abrasive mass flow rate. As an abrasive material, garnet #36 was used, as shown in

Fig. 2. SEM photograph of the abrasive material used (scale = 100 μm).

Table 1
Cutting conditions and process parameters

Parameter	Unit	Range
Traverse rate	mm/s	4.2
Standoff distance	mm	9.0
Pump pressure	MPa	138–345
Abrasive flow rate	g/s	4.3
Abrasive size	mesh	#36
Abrasive particle diameter	μm	485
Abrasive material		Garnet
Impact angle	°	90
Orifice diameter	mm	0.33
Focus diameter	mm	1.02
Focus length	mm	76.2

Fig. 2. Grey cast iron samples were used as the investigated material. The cutting parameters and cutting conditions are listed in Table 1. For catching and collecting the suspension of used abrasives, process water and removed wear particles, a special collection unit was developed which consists primarily of a closed Plexiglas chamber. After cutting, the suspension was removed from the chamber and dried at room temperature. After drying, the cast iron particles and the abrasive grains were separated using a magnet. This process was controlled by periodic inspections using scanning electron microscopy (SEM) and energy dispersive spectroscopy (EDS) measurements. In order to estimate the grain distributions of the collected wear particle samples, sieve analyses were carried out. The particle movement during sieving was performed by a commercial sieve shaker. To estimate the efficiency parameters α and μ in Eqs. (1) and (2) impact-force measurements were performed on plain water jets and abrasive water jets, as described in Ref. [11].

4. Results

4.1. Material volume removal

Fig. 3 shows the relationship between the applied pump pressure, p, and removed cast iron volume, V_D. It can be seen from Fig. 3 that the removed material volume increases linearly with rising pressure, following the relationship:

$$V_D = C_1 (p - p_C) \tag{10}$$

The intersection between the function and the pressure axis can be identified as a critical threshold pressure, p_C. Beyond this pressure range (in this case $p_C < 60$ MPa) no material removal is possible. This threshold value depends strongly on the traverse rate, V_T, but it can be applied as a material constant if it is estimated under identical process conditions. From Fig.

3 it can be concluded that the removal efficiency tends to decrease at comparatively high pressures (in this case $p > 300$ MPa). This observation is in agreement with trends measured in abrasive water-jet cutting experiments at very high pressures by other researchers [29]. Probably, the cutting process becomes ineffective beyond this pressure range because of a decreased mixing and acceleration efficiency. Based on impact-force measurement on plain and abrasive water jets, it was shown in Refs. [11,30] that the efficiency of the energy transformation in water-jet orifices and in abrasive water-jet mixing nozzles starts to drop beyond a particular pump pressure: this may generate the drop in the progress of the depth of cut function at comparatively high pump pressures.

4.2. Average wear particle diameter

A SEM image of a mixture of removed cast iron particles and broken abrasive particles is shown in Fig. 4. Significant differences can be noticed in the surface structures of both materials. The broken abrasive grains, marked as 'A', exhibit large smooth fract areas, indicating unrestrained crack growth. Considering the different magnifications in Figs. 2 and 4, the size reduction during the mixing and cutting process is well documented. The basic mechanism of this size reduction is obviously impact comminution due to impact contact between the abrasive particles and the focus wall or the material sample surface [26]. The cast iron wear particles marked as 'B' in Fig. 4 also generally show features of brittle fracture. But in contrast to the abrasive material, the size of the fracture areas are much smaller, which indicates a mixed material removal mode.
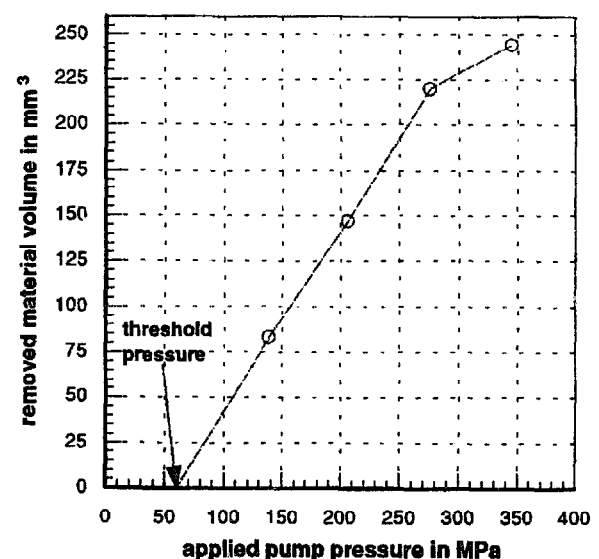

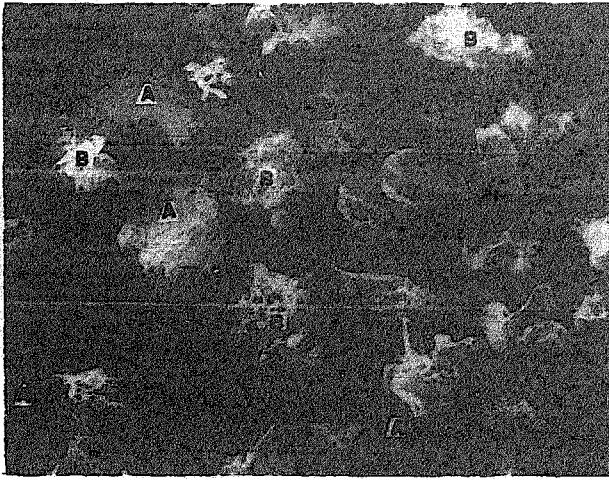Fig. 3. Relationship between the applied pump pressure and the material volume removed.

Fig. 4. SEM photograph of a removed material grain sample (scale: 100 μm, applied pressure: 276 MPa). (a) broken abrasive grains, and (b) removed cast iron grains.

Fig. 5 illustrates the influence of the abrasive velocity, w_p, calculated by Eq. (3) on the average wear particle diameter, D, of the removed cast iron sample. The abrasive particle velocity is used here to compare the estimated wear particle sizes with erosion debris sizes reported from dry solid particle erosion experiments. For the given velocity range, the relationship can be approximated reasonably by a parabolic function. But from the point of view of the physics of the process it can be assumed that the average wear particle diameter, D, cannot exceed the value of $D = 0$ if the abrasive velocity does not reach the threshold velocity ($w_c = 130$ m/s), which means $w_p < w_c$. This assumption indicates that a maximum wear particle diameter may
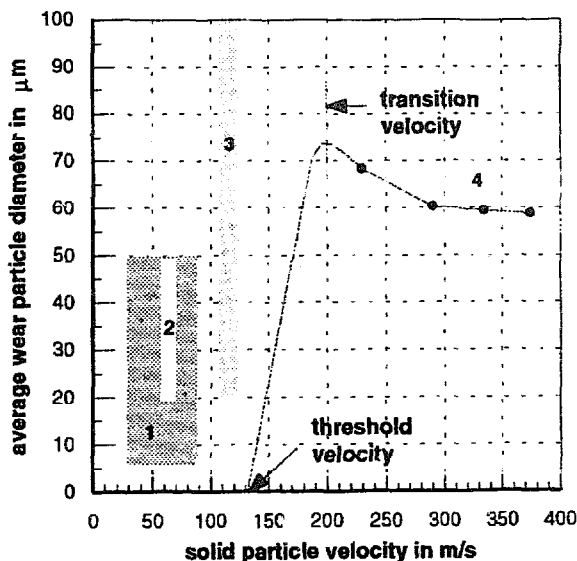

Fig. 5. Relationship between the solid particle velocity and the average wear particle diameter: (1) mild steel, dry solid particle erosion [18]; (2) carbon steel, dry solid particle erosion [19]; (3) hardened steel, dry solid particle erosion [18], and (4) cast iron, abrasive water-jet cutting.

exist at a particular abrasive particle velocity, which latter is marked as a 'transition' velocity at $w_p = 200$ m/s in Fig. 5. Below this velocity level the wear particle size increases almost linearly with increasing particle velocity. Beyond the transition velocity the wear particle size starts to drop with a further increase in the abrasive particle velocity. Generally, the wear debris size is comparable with that observed during the dry solid particle erosion of metallic surfaces, as illustrated on the left section of Fig. 5.

4.3. Influence of pump pressure and abrasive particle velocity on the contact number

To estimate the direct relationship between the pump pressure and the contact number it is necessary to quantify the sensitivity of the comminution number, χ, defined by Eq. (7), to the applied pump pressure. Therefore, a regression analysis of results published in Ref. [26] was carried out, the regression giving:

$$\chi = C_2 \ln p - C_3 \tag{11}$$

For the pressure range applied in this study the values for the comminution number are between $\chi = 0.65$ and $\chi = 0.95$. In a previous study [7] it was found that the average grain size of a brittle material, as estimated by Eq. (9) removed by abrasive water jets in the given pressure rang, can be related to the pump pressure by Eq. (11):

$$D = C_4 p^{-1.5} \tag{12}$$

Based on Eqs. (10)–(12), the contact number, C_N, can be estimated as a function of the applied pump pressure:

$$C_N = \frac{C_1 r_1 d_p^3 \rho_p (p - p_c)}{M_p L_K (C_4 p^{-1.5})^3 [1 + (C_2 \ln p - C_3)]} \tag{13}$$

Eq. (13) indicates a complex relationship between both parameters. The results of calculations based on Eq. (13) as well as on the experimentally estimated values for d_p, M_p, L_K and p_c are presented in Fig. 6 together with the measured contact numbers, including abrasive particle fragmentation effects. The global relationship between the pump pressure and the contact number $C_N = f(p)$, is non-linear. A drop in the function at very high pump pressures can be noticed again, which indicates critical machining conditions existing at a particular pressure level. It seems from Fig. 6 that a 'saturation' contact number, $C_{N.max}$, may exist which will be obtained at very high pressure levels. Interestingly, in the range of medium pump pressures ($p = 150$–300 MPa) the relationship between the pump pressure and the contact number is linear.

The range of the estimated contact numbers lies between $C_N = 3$ and $C_N = 11$. These values are fairly high compared with contact numbers estimated for dry solid particle erosion of metals. To compare abrasive
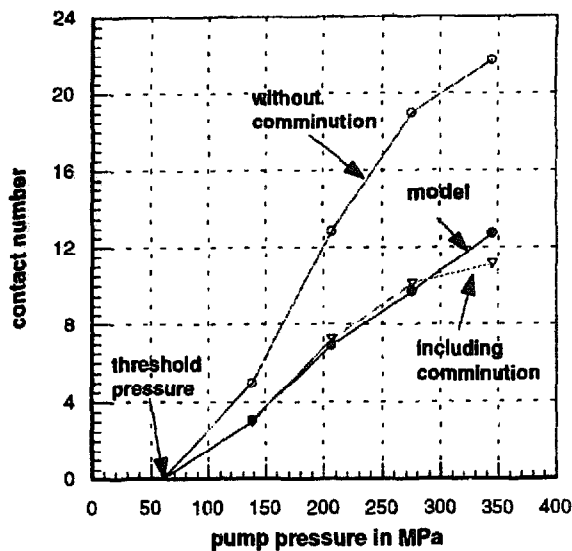
Fig. 6. Relationship between the applied pump pressure and the estimated contact number.

water-jet cutting and dry solid particle erosion, the relationships between the contact numbers and the particle velocities are plotted in Fig. 7. As shown in this figure, contact number values of $C_N = 0.1-0.25$ for soft steel, and values between $C_N = 0.5-1.0$ for hardened steel eroded by solid particles were found. For the erosion of carbon steel, which showed some features of brittle fracture, contact numbers of $C_N = 0.2-0.6$ were detected [19]. Generally, the contact numbers for solid particle erosion are lower than $C_N = 1$, suggesting a
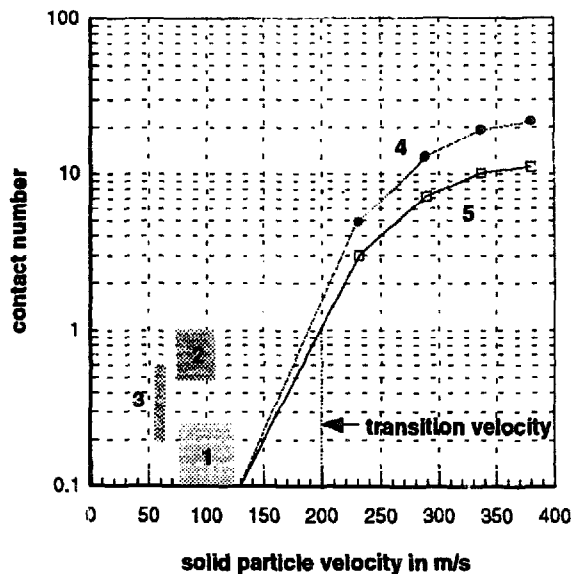

Fig. 7. Relationship between the solid particle velocity and the contact number for dry erosion and abrasive water-jet erosion: (1) mild steel, dry solid particle erosion [18]; (2) hardened steel, dry solid particle erosion [18]; (3) carbon steel, dry solid particle erosion [19]; (4 and 5) grey cast iron, abrasive water-jet cutting; (4) without abrasive particle comminution, and (5) including abrasive particle comminution.

cumulative solid particle impact that may be necessary to remove an erosive wear particle. For the abrasive water-jet cutting process, it is again assumed that no debris can be removed if the particle velocity is lower than the threshold velocity, $w_P < w_C$. It can be noted that under this condition the contact number function crosses the $C_N = 1$-line at the particle velocity of $w_P = 200$ m/s, which is identical to the 'transition' velocity noticed in Fig. 5.

5. Discussion

The state-of-the-art analysis of the abrasive water-jet cutting process generally neglects a direct action of the high-speed water on the material surface [31,32], the water jet being considered only as an accelerator for the abrasive particles. This assumption has been validated for a wide range of metallic materials which cannot be cut by plain water jets, but in contrast, pre-cracked materials and materials containing a particular degree of instabilities, such as microcracks and pores, can be cut effectively with plain water jets at commercial pressure ranges [33]. In a classical experiment [34] it was shown that a pre-cracked material cannot be damaged by a plain water jet if it is covered by a very thin metal layer which prevents the high velocity water flow from entering the cracks and pores. If the layer is removed the material fails by internal stresses created in the material by the penetrating water stream. As suggested in Refs. [33,36], the water enters a crack with high velocities and generates stresses on the crack walls. When the intensity of these stresses exceeds critical local material resistance parameters, such as fracture toughness, the crack will be widened. An intersection of several cracks leads to the formation of a microcrack network and the generation of wear particles. It was shown in Refs. [33,37] for the water-jet cutting of materials that:

$$w_{cr} \propto K_{Ic} = \frac{K_{Ic}}{\sqrt{2\pi l_{cr}}} \tag{14}$$

where w_{cr} is the critical threshold velocity of the water flow. For an undamaged material with $l_{cr} = 0$, the threshold water-jet velocity, w_{cr}, is infinite and the material cannot be cut. However, the water threshold velocity can be reduced significantly when cutting a material containing flaws and cracks. Grey cast iron contains some instabilities because of the graphite flakes in the structure. Nevertheless, undamaged cast iron usually cannot be cut by plain water jets. This situation may change if a particular number of surface cracks is present which can be entered by the high-speed water flow. The formation of surface cracks during the erosion of grey cast iron by solid particles was observed in Ref. [25]. These cracks were still

present during post-erosion SEM inspection, indicating that no additional force was present to widen and intersect them. Therefore, several particle impacts are necessary to remove material debris under this condition. This means that $C_N < 1$ which is in fact the situation in the abrasive water-jet cutting of grey cast iron with jet velocities below the 'transition' velocity, $w_p < 200$ m/s. In this range, the water velocity is not high enough to widen the cracks generated by the abrasive particle impact: thus, Eq. (14) is not satisfied. Increasing the jet velocity beyond the 'transition' velocity, $w_p < 200$ m/s, it can first be assumed that the lengths of the generated crack will increase. Additionally, the water flow velocity will increase. A particular combination of both effects will satisfy Eq. (14), which allows the water flow to contribute directly to the material removal process. The water can open isolated cracks and create a crack network. The embedded graphite flakes will reinforce this process, as shown in Ref. [20] for cavitation erosion. This process shows some similarities to a dynamic fragmentation process [7]. Assuming this, the average fragment size will be reduced with increasing loading intensity [38]: this is well illustrated in Fig. 5. With increasing material removal rate and a decrease in the average wear particle size, the number of removed target particles must increase, yielding larger contact numbers with higher pump pressures, as shown in Fig. 6.

The phenomenologic model supposed above was suggested independently by observations in photo-elastic materials subjected to abrasive water jets. In Ref. [39], the authors concluded from photo-elastic and SEM studies that an incessant bombardment of abrasive particles created crack nucleation sites with crack growth abetted by the hydro-wedge action of the oncoming water jet.

6. Conclusions

In this study, investigations on wear particles generated during the cutting of grey cast iron by abrasive water jets were carried out, the results leading to the following conclusions.

1. An experimental method, based on the sieve analysis of the removed wear particles, can be used to estimate the contact numbers for the abrasive water-jet erosion process in grey cast iron.

2. The material-removal process is characterized by a threshold pump pressure, p_C, and a threshold abrasive particle velocity, w_C.

3. The material-removal efficiency is reduced at very high pump pressures and abrasive particle velocities.

4. The average diameter of the debris removed by the abrasive water jet has a maximum value at a particular 'transition' particle velocity.

5. The estimated contact numbers are in the range of $C_N = 3-11$, which is higher than the contact numbers estimated for dry solid particle impact erosion.

6. The contact number increases with the abrasive particle velocity, for low and average particle velocities ($w_p = 200-350$ m/s) the relationship between abrasive particle velocity and contact number being linear, while for lower and higher particle velocities the progression of the curve decreases.

7. A phenomenologic model for a complex material-removal mechanism is supposed combining the effects of solid particle impact phenomena and the erosive action of the high-speed water flow.

7. List of symbols

C_{1-5}	constants
C_N	contact number
d_o	sieve diameter for 0.1% overflow
D	average wear particle diameter
d_p	average abrasive particle diameter
d_u	sieve diameter for 99.9% overflow
d'	grain size distribution parameter
d_w	water orifice diameter
K_{1c}	critical stress intensity factor
l_{cr}	critical crack length
L_K	length of the cut
m_D	mass of a single wear particle
m_p	mass of a single abrasive particle
M_D	mass removal
$\dot{M}_p$	abrasive flow rate
$\dot{M}_w$	water flow rate
n	grain size distribution parameter
N_D	number of removed wear particles
N_p	number of abrasive particles
p	applied pump pressure
p_C	threshold pump pressure
t_E	exposure time
v_r	traverse rate
V_D	volume removal
w_o	water jet velocity
w_C	abrasive particle threshold velocity
w_{CI}	water-jet threshold velocity
w_p	abrasive particle velocity

Greek letters

α	abrasive focus efficiency parameter
χ	comminution number
μ	water orifice efficiency number
ρ_p	abrasive material density
ρ_w	water density

Acknowledgements

References

[1] H. Hochheng and K.R. Chang, J. Mater. Proc. Technol., 40 (1994) 287–307.

[2] A. Momber, I. Eusch and R. Kovacevic, 8th American Water Jet Conf., Houston, TX, USA, 1995, pp. 229–244.

[3] D. Arola and M. Ramulu, Proc. 7th American Water Jet Conf., Seattle, WA, USA, 1993, pp. 43–64.

[4] A. Momber, Beton Stahlbetonbau, 89 (1994) 132–134.

[5] A. Laurinat, H. Haferkamp and H. Louis, Maschinenmarkt, 99 (1993) 22–27.

[6] A. Momber, Handbuch Druckwasserstrahl-Technik. Beton Verlag, Düsseldorf, 1st edn., 1993.

[7] A. Momber, H. Kwak and R. Kovacevic, ASME J. Tribol., 118 (1996) in press.

[8] R. Mohan, A. Momber and R. Kovacevic, ASME Med. 2-1, 1995, pp. 69–85.

[9] A. Momber, R. Kovacevic, H. Kwak and R. Mohan, 8th American Water Jet Conf., Houston, TX, USA, 1995, pp. 187–206.

[10] A. Momber and R. Kovacevic, Manufacturing Science and Engineering, Vol. 1, American Society for Mechanical Engineering, New York, 1994, pp. 361–366.

[11] A. Momber and R. Kovacevic, ASME HTD-231/FED-233, 1995, pp. 243–256.

[12] E. Nadeau, G.D. Stubley and D.J. Burns, Int. J. Water Jet Technol., 1 (1991) 109–116.

[13] G. Zhou, M. Leu, E. Geskin, Y.C. Chung and J. Chao, ASME PED, 62, 1992, pp. 191–202.

[14] S.P. Raju and M. Ramulu, Manufacturing Science and Engineering, Vol. 1, American Society of Mechanical Engineering, New York, 1994, pp. 339–351.

[15] A. Momber and R. Kovacevic, Inst. Mech. Eng., J. Manuf. Eng., 209 (1995) 491–498.

[16] A. Momber, 8th American Water Jet Conf., Houston, TX, USA, 1995, pp. 829–843.

[17] J. Kleis and U. Uuemois, Z. Werkstofftech., 5 (1974) 381–389.

[18] S. Tscherny, E. Wandke and U. Frohner, Schmierungstech., 19 (1988) 235–239.

[19] A. Hammarsten, S. Soderberg and S. Hogmark, Wear of Materials, American Society of Mechanical Engineering, New York, 1982, pp. 373–381.

[20] T. Okada, Y. Iwai and A. Yamamoto, Wear, 84 (1983) 297–312.

[21] I.R. Sare, B.K. Arnold, G.A. Dunlop and P.G. Lloyd, Wear, 162–164 (1993) 790–801.

[22] I.R. Sare and B.K. Arnold, Wear, 131 (1989) 15–38.

[23] G. Laird, W.K. Collins and R. Blickensderfer, Wear, 124 (1988) 217–235.

[24] A. Wang, U.J. de Souza and H.J. Rack, Wear, 151 (1991) 157–173.

[25] K.P. Balan, V. Redy, V. Joshi and G. Sundararajan, Wear, 145 (1991) 283–296.

[26] M. Simpson, Int. J. Water Jet Technol., 1 (1990) 17–28.

[27] T.J. Labus, K.F. Neusen, D.G. Albers and T.J. Gores, J. Eng. Ind., 113 (1991) 402–411.

[28] H. Schubert, Aufbereitung fester mineralischer Rohstoffe, Vol. 1, VEB Deutscher Verlag für Grundstoffindustrie, Leipzig, 1988.

[29] K. Faber and H. Oweinah, Jet Cutting Technology, Elsevier Applied Science, London, 1991, pp. 365–382.

[30] M. Hashish, J. Eng. Mater. Technol., 111 (1989) 221–228.

[31] M. Hashish, Proc. 7th Int. Conf. Jet Cutting Technology, BHRA Fluid Engineering, Cranfield, UK, 1984, pp. 249–265.

[32] M. Mazurkiewicz, SME Tech. Paper MS 89-811, Society of Manufacturing Engineers, Dearborn, MI, pp. 1–15.

[33] A. Momber and R. Kovacevic, Int. J. Fract., 71 (1995) 1–14.

[34] S.E. Forman and G.A. Secor, Soc. Petr. Eng. J., 14 (1974) 10–18.

[35] A. Momber, R. Kovacevic and J. Ye, Tribol. Trans., 38 (1995) 686–692.

[36] A. Momber and R. Kovacevic, J. Mater. Sci., 31 (1996) 1081–1085.

[37] J. Wiedemeier, Ph. D. Thesis, University of Hannover, Germany, 1981.

[38] D.E. Grady, J. Appl. Phys., 53 (1982) 322–325.

[39] M. Ramulu, H. Yeh, K.P. Wong and S.P. Raju, Proc. 6th American Water Jet Conf., Water Jet Technology Association, St. Louis, MO, 1991, pp. 1–15.